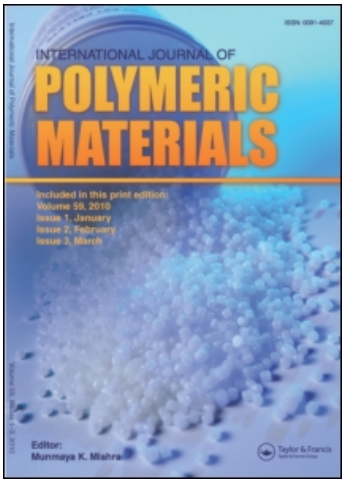

International Journal of Polymeric Materials
Publication details, including instructions for authors and subscription information:
http://www.informaworld.com/smpp/title~content=t713647664

Nanostructure of Potato Starch, Part I: Early Stages of Retrogradation of Amorphous Starch in Humid Atmosphere as Revealed by Simultaneous SAXS and WAXS

R. K. Bayer[a]; F. J. Baltá-Calleja[a]
[a] Instituto de Estructura de la Materia, CSIC, Madrid, Spain

To cite this Article Bayer, R. K. and Baltá-Calleja, F. J.(2006) 'Nanostructure of Potato Starch, Part I: Early Stages of Retrogradation of Amorphous Starch in Humid Atmosphere as Revealed by Simultaneous SAXS and WAXS', International Journal of Polymeric Materials, 55: 10, 773 — 788
To link to this Article: DOI: 10.1080/00914030500440229
URL: http://dx.doi.org/10.1080/00914030500440229

International Journal of Polymeric Materials, 55:773–788, 2006

ISSN: 0091-4037 print/1563-5333 online
DOI: 10.1080/00914030500440229

Taylor & Francis
Taylor & Francis Group

Nanostructure of Potato Starch, Part I: Early Stages of Retrogradation of Amorphous Starch in Humid Atmosphere as Revealed by Simultaneous SAXS and WAXS

R. K. Bayer
F. J. Baltá-Calleja
Instituto de Estructura de la Materia, CSIC, Madrid, Spain

Crystallization experiments on amorphous, injection-molded starch in a humid atmosphere are reported. The crystallization mechanisms have been studied using simultaneous SAXS and WAXS during a temperature stepwise increase. In contrast to the crystallization of linear synthetic polymers, in starch the WAXS peaks are observed at low temperature before the appearance of the SAXS maximum. The initial state of crystallization is dominated by the amylose (AM) component of the potato starch alone. After the initial formation of large (16 nm) uncoordinated individual crystallites, stacks of lamellae and finally, an insertion of thinner lamellae within the stacks are observed. Results indicate that only if all AM is converted into a semicrystalline structure and if the secondary starch network of double helices of AM and amylopectin (AP) is molten by a temperature increase above 70°C, crystallization of AP also occurs. Because the AM crystals act as nuclei for the AP component, a common superstructure is developed. Within a spherulite, alternating AM and AP lamellae develop radially from the center of the AP molecule. Results suggest that the AM is distributed inhomogeneously with respect to the AP molecules, leaving approximately one half of the AP fraction free, which means not crystallized to a spherulitic structure together with AM.

Received 20 October 2005; in final form 31 October 2005.

Grateful acknowledgment is due to the MEC, Spain (grant FIS2004-01331) for the generous support of this work. RKB gratefully acknowledges the Secretaría de Estado de Universidades e Investigación, MEC, and the "European Social Fund" for the award of a Sabbatical Grant (SAB2003-0131). RKB also thanks the DFG (Deutsche Forschungsgemeinschaft) for the support of this work. The SAXS and WAXS data discussed in this work were derived from measurements carried out at HASYLAB, DESY, Hamburg, under project II-04-029 EC. The IHP-Contract HPRI-CT-1999-00040 of the European Community funded this project. The Arburg Company in Lossburg, Germany is thanked for the kind supply of the injection-molding machine used.

Present address: R. K. Bayer, Universität Kassel, Mönchebergstr.3, D-34125 Kassel, Germany.

Address correspondence to F. J. Baltá-Calleja, Instituto de Estructura de la Materia, CSIC, Serrano 119, 28006 Madrid, Spain. E-mail: embalta@iem.cfmac.csic.es

Keywords: amorphous starch, nanostructure development, retrogradation, SAXS, WAXS

INTRODUCTION

Potato starch consists of 25% amylose (AM) and 75% amylopectin (AP). On the basis of this composition, potato starch appears as suitable material to investigate the early stages of the crystallization of AP induced by AM [1]. When the AM content is very low, its nucleation efficiency is not so high. From 25% on upward, amylose seems to be a good nucleation agent for the AP crystallization [2]. Rindlav-Westling has pointed out that the crystallization of AM is much faster than that of the AP under the same conditions [3]. A preceding article has shown that the early stages of crystallization of potato starch are characterized by the entanglement network of AM [4]. Hence it can be assumed that the beginning of the crystallization of potato starch is controlled only by AM.

Starch crystals are mainly formed by double helices, both from AM and AP. In the presence of a fat, as it is the case for many native starch substances (i.e., corn starch), amylose—lipid complexes (AL–complex) are formed. AM molecules that participate in AL–complexes, do not participate in double helix formation, which is a self-complexing mechanism. A chain-sequence cannot take part simultaneously in two different complexes. For example, gelatinization of starch, which takes place through double helix formation, is severely hindered by the presence of fat [5–6]. Potato-starch has the advantage that it does not contain any fat. Therefore, this starch is an especially suitable candidate for the development of crystallinity. The AP fraction of potato starch is available with sufficiently long chain-end bundles favoring crystallization [7]. This peculiarity of potato starch also explains, in comparison to AM rich starch, its unusual high gelatinization enthalpy. One can follow the early stages of crystallization, if one starts the experiment with completely amorphous potato starch, which can easily be prepared by injection molding [8–9]. Crystallization can be induced by storage in a humid atmosphere [10].

The aim of the present work is the study of the early stages by means of simultaneous WAXS and SAXS. A second part begins the other way round from an already perfectly retrogradaded potato starch gel. The initial state of the crystallization is approached in this case by successive melting of the highly organized crystal-structure.

EXPERIMENTAL

Materials and Thermal Treatment

Potato starch samples were injection molded (employing an ARBURG-All rounder 250S) using the elongational-flow method [8–9], which yields ductile-oriented amorphous materials. A melt temperature of 140°C and a molding temperature of 25°C were used, respectively. The molded samples were kept at ambient atmosphere, leading to a humidity of 12%. For the WAXS experiments 1-mm thick cuts were prepared. The air-conditioned samples were brought into water-saturated atmosphere inside sealed glass tubes at room temperature and heated at 40, 69, 88, and 94°C, respectively, for periods of 10 min each. The lower part of the tubes was filled with a small amount of water whereas the sample was placed in the upper part, thus avoiding contact with the water surface.

Techniques

Wide-angle X-ray scattering experiments (WAXS) were performed using a double focusing camera adapted to the synchrotron radiation source at the beamline A2 in HASYLAB, DESY, Hamburg. The wavelength used was 0.15 nm (8 keV) with a band pass of $dl/l = 5.10^{-5}$. Scattering patterns were recorded every 30 s using a linear position-sensitive detector. The patterns were corrected for fluctuations in intensity of the primary beam and for the background. The accumulation time per frame was 30 s. The integral breadth of the reflections $d\beta$ was directly measured from the experimental profile to make an estimate of the value for the coherently diffracting domains $D \cong 1/d\beta$, normal to the chain direction as a function of temperature. The evaluations refer to previously reported SAXS and WAXS experiments [11].

In the present study the long period (L), the size of the coherently diffracting domains (D), the SAXS invariant (Q), the total degree of crystallinity (X_c), the degree of crystallinity within the lamellar stacks (X_{cL}), and the fraction of lamellar stacks within the spherulite (X_L) are discussed.

RESULTS AND DISCUSSION

Crystallization Mechanism of Amylose

Figures 1a and b illustrate the development of the total crystallinity, X_c, the crystallinity within the lamellar stacks, X_{cL}, and the fraction

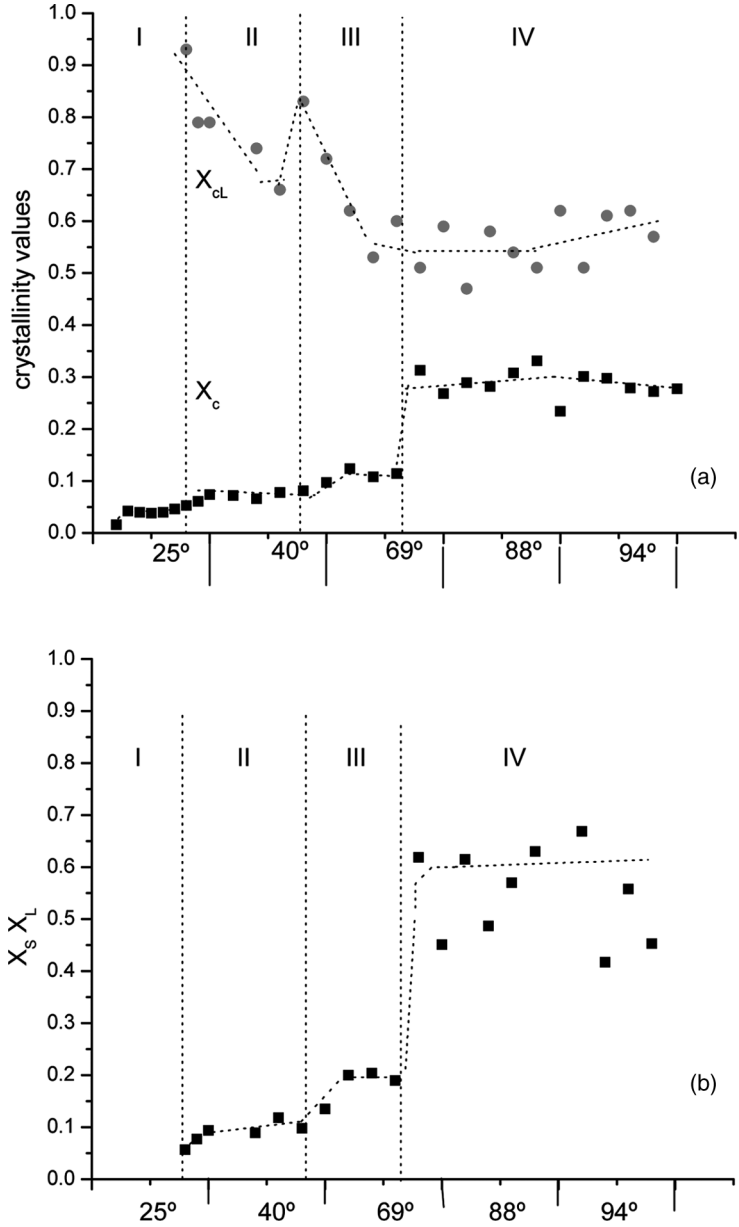

FIGURE 1 Variation of (a) total crystallinity, X_c, and crystallinity within the lamellar stacks, X_{cL} of initially amorphous potato starch as a function of temperature in humid atmosphere. Every temperature step takes 10 min and (b) fraction of crystallized lamellar stacks, $X_S X_L$, with increasing temperature.

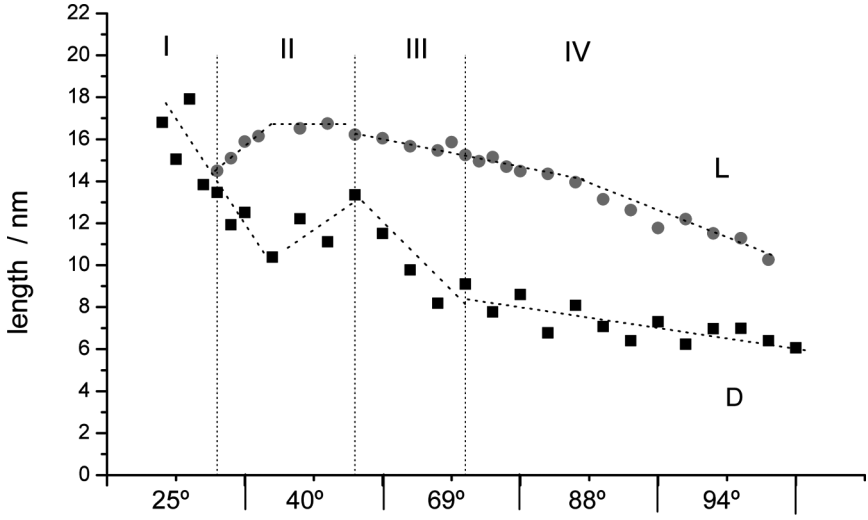

FIGURE 2 Variation of long-period L and lateral size of crystal blocks, D, of initially amorphous potato starch in humid atmosphere as a function of the time–temperature program.

of crystallized lamellar stacks, $X_S X_{L,}$ as a function of increasing temperature. Accordingly, four regions (I, II, III, IV) can be distinguished. These four regions can be also discussed in light of other structural quantities: L, D, Q, and $\Delta\rho^2$, derived from SAXS and WAXS (see Figures 2 and 3). The first crystals from AM observed in region I are not regularly packed in a periodic order. Consequently, the quantities X_{cL} and $X_S X_L$ cannot be defined in this region. In regions II and III X_c shows a slight stepwise increase. At the beginning of region IV the crystallinity exhibits a much stronger increase. In Reference [10] it was shown that the diffusion of water into amorphous starch first leads to a linear crystallinity increase over the square root of time leaving the amorphous phase still dry (diffusion mechanism 1, up to approximately 14%). Thereafter a strong increase of diffusion takes place, wetting the amorphous regions too (diffusion mechanism 2). This leads to a strong X_c increase. It seems reasonable, that the X_c–step between regions III and IV may correspond to this transition.

Figure 2 also indicates that water diffusion into the crystals (diffusion mechanism 1, [10]) yields three different morphologies (regions I to III).

Up to $X_c = 5\%$ only uncoordinated large crystal blocks (up to 18 nm) are formed (see Figures 1 and 2). The first crystals are built up by

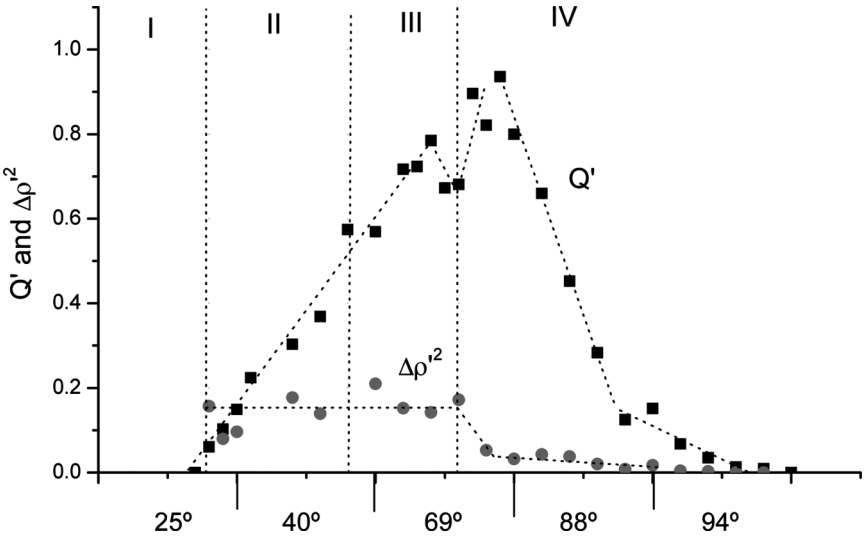

FIGURE 3 The invariant Q' of SAXS and electron density fluctuation $\Delta\rho'^2$ as a function of the time–temperature program for initially amorphous injection molded potato starch in humid atmosphere.

penetration of water into zones of AM, particularly suitable for crystallization, where it is bound as crystal water [10]. Humid amorphous zones do not exist; interpenetrated water is directly transformed into a crystal block. Crystal blocks are distributed without any order within a dry amorphous matrix. Figure 3 shows that the electron density fluctuation $\Delta\rho^2 \sim (\rho_c - \rho_a)^2$ remains constant at regions I to III; that is, neither ρ_c nor ρ_a change. This result fits well to the earlier conclusion that water does not penetrate into the amorphous regions before the transition to region IV is reached. If one considers the amorphous AM to be formed by blobs of chains [12] (a blob is a mesh of the entanglement network, interpenetrated by other meshes of AM chains), then the entanglement free-zone within the blob can be regarded as a precursor of the crystal. From preceding studies [4] the dimensions of an averages blob are of about 15 nm, which agrees well with a thickness of 18 nm for the largest crystals. This value is higher than the largest long period observed (see Figure 2). With increasing time the newly formed crystallites becomes smaller, whereas the overall crystallinity only gradually increases. When crystal dimensions of $D = 13.5$ nm are reached (at the transition from I to II, Figure 2), these more mobile blocks can arrange themselves into stacks of crystal lamellae, giving rise to a stacking periodicity of $L = 14.4$ nm.

At 40°C (zone II), a significant increase is superimposed on the continuous decrease of D leading at the end of region II to a maximum in D, as well as in L. Apparently the periodicity of stacks of lamellae represents a nucleation step, because X_c rises gradually at the transition between I and II from 5 to 8% (see Figure 1a). The distinct increment of D represents an anomaly. In other words, mainly thick crystals are formed when crystallization starts, whereas smaller crystals are built up when crystallization proceeds, that is, in the case of AM when water penetrates into less perfect blobs. This explains the course of the curve in range I (Figure 2). The anomalous increase of L and D at the end of region II is discussed in what follows.

According to Strobl's crystallization model a lamellar structure develops from preexisting crystal blocks [13]. The molecular mobility in range II causes that also the randomly distributed thick blocks of region I are now arranged into the lamellar crystals. The newly formed crystals can now develop into thicker crystalline lamellae, giving rise to a D and L increase in region II.

In range II, $X_S X_L$ increases only slightly with respect to X_c corresponding to still well-organized crystal blocks (linear crystallinity X_{cL} close to 1). Only few lamellar stacks with high crystalline perfection are embedded in an amorphous matrix.

In zone III, crystallinity further increases, whereas the long period and D drop. This is typical for the insertion of thinner crystals into the interspaces between thicker lamellae, which are formed earlier. This is just the normally expected behavior. In this case, some water presumably enters the amorphous zones within the lamellar stack, generating new thinner inter-lamellar zones. The perfection of the crystals, described by the linear crystallinity X_{cL}, now decreases strongly (down to 0.6).

Summarizing; the areas I to III emerge from each other. Thus, region I is characterized by the presence of the first uncoordinated thick AM crystallites. In region II an arrangement of these blocks into a periodic lamellar structure occurs. Finally, region III characterizes the insertion of thinner lamellar within the inter-lamellar amorphous zones of structure II.

Hence, it seems reasonable to think that all three regions refer to the crystallization of AM alone, which is characterized by the absorption of water into the crystalline zones, leaving the remaining amorphous regions in a dry state. Proof in support of this is found by the fact that $X_S X_L$ is close to 20% at the end of range III. This is the volume fraction of semicrystalline material, which approaches the AM content in potato starch. At the end of region III, the crystallization of AM must come inevitably to an end, because nearly all AM molecules

are incorporated into an alternating crystalline–amorphous layer structure. Additional information is provided by the X_{cL} (X_c) plots later in the article.

Crystallization of Amylopectin

In range IV the water progressively penetrates into the amorphous regions. This is caused by the thermal dissociation of the secondary network, approximately at 60°C, which increases the molecular mobility in the amorphous phase. This phenomenon is described [10] through the penetration of "free" water (diffusion region 2), which is not as strongly bound as crystal water. In this case, not only the inter-lamellar zones but also the amorphous regions between the lamellar stacks, as well as the amorphous inter-spherulitic regions, being both characterized by $(1 - X_L X_S)$, are affected by the crystallization. Large amorphous regions are now transformed into partially crystalline zones. At the beginning of crystallization region IV, X_c steps from 12% up to 30%, whereas $X_S X_L$ rises from 20% up to 60% (Figure 1b), clearly contributing to the decrease of the amorphous phase $(1 - X_S X_L)$. Because at this time all AM is crystallized, the range IV of crystallization should be connected to that of AP. In a previous study [14], it was observed that within injection molded potato starch the AP molecules are interpenetrated by the AM network in an inhomogeneous manner. Especially AM concentrates in one third of all AP molecules and stabilizes them against solubility in water by bonding to a secondary network. The remaining two thirds of AP molecules dissolve easily in water. According to Reference [15] the solubility is influenced by the degree of branching. Probably these AP molecules present denser branching zones, which on the one hand makes them less capable of being interpenetrated by AM. On the other hand the branching zones make them more resistant to crystallization. One can, therefore, assume that the AP of potato starch will crystallize in two steps: Firstly one third of the material crystallizes, because the AP molecules contain less branches and due to the nucleation of a high number of AM crystals within the AP volume. Because the AM fraction amounts to approximately 25%, in the first step approximately 50% of the material should crystallize (one third of the potato starch AP corresponds to 25% of the total volume). This expectation is confirmed in Figure 1b. At the beginning of the region IV, $X_S X_L$ increases rapidly up to a fraction of approximately 50–60%, which levels off thereafter. The remaining 40–50% of the material (mainly AP) crystallizes in a second step, which requires a longer time period (at least 2 days) at room temperature [16–17].

The experiments presented here leave that fraction of starch in the uncrystallized, amorphous state.

In region IV the crystal perfection X_{cL} does not change anymore, remaining at a low level of approximately 0.55. The AP crystals apparently become inserted into the crystalline stacks of AM, because both L as well as D further decrease in range IV. Hence, the single AP lamellae insert themselves between the preexisting AM crystal stacks. The overall crystallinity (X_c) immediately rises in range IV up to 30%. Because the crystallization refers to approximately one half of the material, the semicrystalline fraction of the AM – AP mixed superstructure amounts already to about 60%. In the case of a complete crystallization in a humid atmosphere, during 20 days at room temperature, no further increase of AM – AP common crystallization is reported [17].

The diffusion of water into the amorphous regions leads to decrease of the amorphous density ($\rho_a = 1{,}48\,g/cm^3$ after storage at room atmosphere [10]), which finally results in a crystalline density $\rho_c = 1{,}42\,g/cm^3$ for the B–crystal; that is, $\Delta\rho^2 \sim (\rho_c - \rho_a)^2 \to 0$, (see Figure 3) whereas the total crystallinity remains unaltered ($X_c = 30\%$, see Figure 1a). This is the reason why the invariant Q' should approach zero, in spite of the absence of melting. A plot of this quantity as a function of crystallinity corroborates the expected behavior (Figure 4).

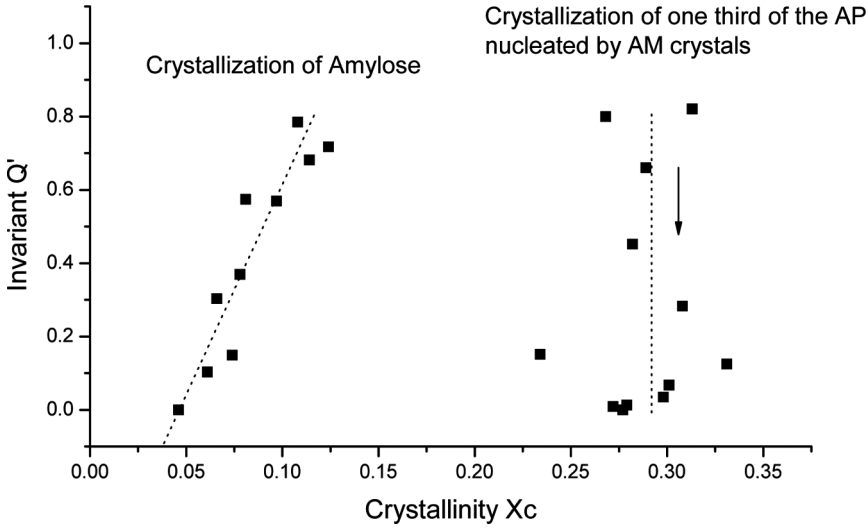

FIGURE 4 Dependence of the invariant Q' upon crystallinity for room atmosphere conditioned initially amorphous potato starch in humid atmosphere.

Figure 4 additionally shows a linear increase of the SAXS-invariant Q' with increasing X_c and an intercept of the abscissa at $Q' = 0$ of 3–4%. This corresponds to the transition of disordered to lamellar organized crystallization (Figure 2). Referring to the content of AM, approximately 15% of the AM must be crystallized before the blocks start to organize themselves into lamellae. At $X_c = 30\%$, Q' falls vertically from its maximum value to zero, in accordance with the approach of ρ_a towards ρ_c, as discussed earlier.

X_{cL} (X_c) Plots as Key to the Understanding of Different Crystallization-Steps

Basic Concepts Relating to the Variation of X_{cL} and X_S X_L with X_c

Concerning the variation of X_{cL} with X_c: at individual nucleation points, spherulitic crystallization may start by formation of stacks of lamellar crystals extending radially from the nucleation center. The first crystal lamellae are of high perfection, that is, their linear crystallinity X_{cL} is close to 1 (the crystals are surrounded by only very thin amorphous layers). Upon further crystal-growth, spherulites finally cover the whole volume of the sample, ($X_S \rightarrow 1$), by leaving gaps between the lamellae stacks within the spherulite, which are filled in later ($X_L \rightarrow 1$). The amorphous layers within the lamellar stacks are filled with thinner crystalline lamellae. This leads to a decrease of X_{cL}. If the crystallinity finally attains 50%, the crystals become the percolating phase, that is, every crystalline lamella that is formed from crystal blocks has contact to other lamellar crystals. The situation of the percolation of the crystals at $X_c = 0.5$ thus is characterized by $X_S X_L = 1$.

Because,

$$X_c = X_S X_L X_{cL} \tag{1}$$

it follows: $X_{cL} = 0.5$. If one interpolates X_{cL} (X_c) linearly between the values $X_{cL} = 1$ at $X_c = 0$ and $X_{cL} = 0.5$ at $X_c = 0.5$ then one obtains for X_{cL} (X_c):

$$X_{cL} = 1 - X_c \qquad \text{for } 0 < X_c < 0.5 \tag{2}$$

For $X_c > 0.5$; $X_S X_L$ remains 1 and from Eq. 1 results:

$$X_{cL} = X_c \qquad \text{for } 0.5 < X_c < 1 \tag{3}$$

From Eqs. 1 and 2 yields for $X_S X_L$

$$X_S X_L = \frac{X_c}{(1 - X_c)} \qquad \text{for } 0 < X_c < 0.5 \tag{4a}$$

$$X_S X_L = 1 \qquad \text{for } 0.5 < X_c < 1 \tag{4b}$$

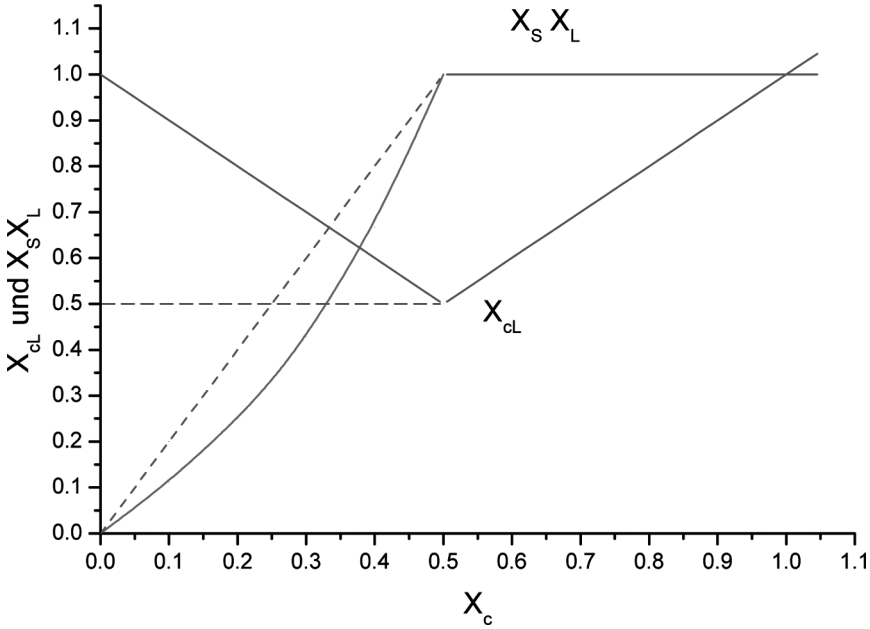

FIGURE 5 Schematic plot of X_{cL} and X_SX_L as a function of X_c.

Figure 5 is a graphic representation of Eqs. 2, 3, and 4a, b.

The quantity X_{cL} (X_c) exhibits a minimum value of 0.5 at $X_c = 0.5$. Larger X_{cL} values are observed for lower as well as for higher X_c. This behavior is characteristic for the described spherulitic type of crystallization; X_{cL} can become smaller than 0.5 only if the crystallization is spherical-shell like, as described for the star-shaped AP molecule [16].

If during the crystallization of starch X_{cL} decreases to a minimum value of 0.5 this is an indicator, on the one hand for the spherulitic type of crystallization, and on the other for the percolation of crystals. The crystals, then, fill the sample volume (primary crystallization) and only a secondary crystallization once more can provide an X_{cL} increase at $X_c > 0.5$.

The horizontal dashed line in Figure 5 describes the case $X_{cL} = 0.5$ for every $X_c < 0.5$.

By inserting $X_{cL} = 0.5$ into Eq. 1 it follows $X_SX_L = 2X_c$, which is the second dashed line in Figure 5. All measured values of X_{cL} for $X_c < 0.5$ should fall into the triangle on the left hand side. The X_SX_L measurements should fit into the narrow bulged area.

Application to the Case of Potato Starch Data

Figure 6 illustrates how the $X_{cL}(X_c)$ and the $X_S X_L(X_c)$ data for the crystallization process of potato starch fit into the postulated framework.

The measurements of X_{cL} as those of $X_S X_L$ both fit into the corresponding areas. The quantity $X_S X_L$, has the character of a master-curve, because the breadth of the bulge area in Figure 5 is rather small. However, in accordance with the two crystallization mechanisms proposed earlier (crystallization of AM and AM – AP), the product $X_{cL}(X_c)$ distinctly exhibits two partial curves, fitting well into the triangle. The transition III–IV in Figure 6 is much better defined than in Figure 2. The common result in both partial curves is that they reach a final value of $X_{cL} = 0.5$, indicating the end of primary crystallization for the two respective mechanisms. If one now relates the final crystallinity $X_c = 0.12$ of the first (AM) mechanism to the AM content of 0.25, a reduced crystallinity $X_c^* = 0.12/0.25 = 0.48 \approx 0.5$ turns out, referring to the AM zones of potato starch alone. It is reasonable, that an end value $X_{cL} \approx 0.5$ is characteristic for that X_c^*. This is a further

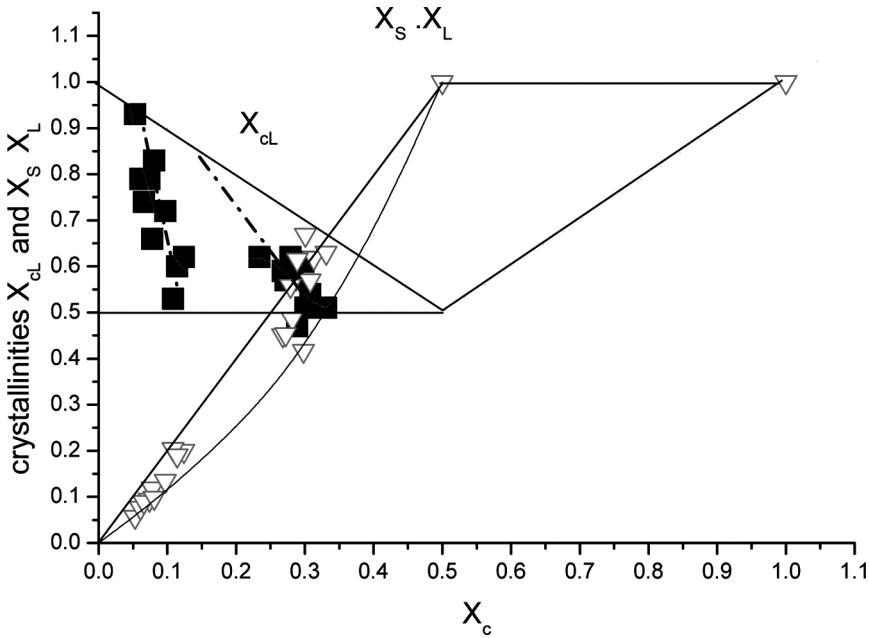

FIGURE 6 Experimental data for linear crystallinity X_{cL} and volume fraction X_S X_L of the semicrystalline zones during the early retrogradation process of initially amorphous starch. Insertion of the data into the framework of Figure 5.

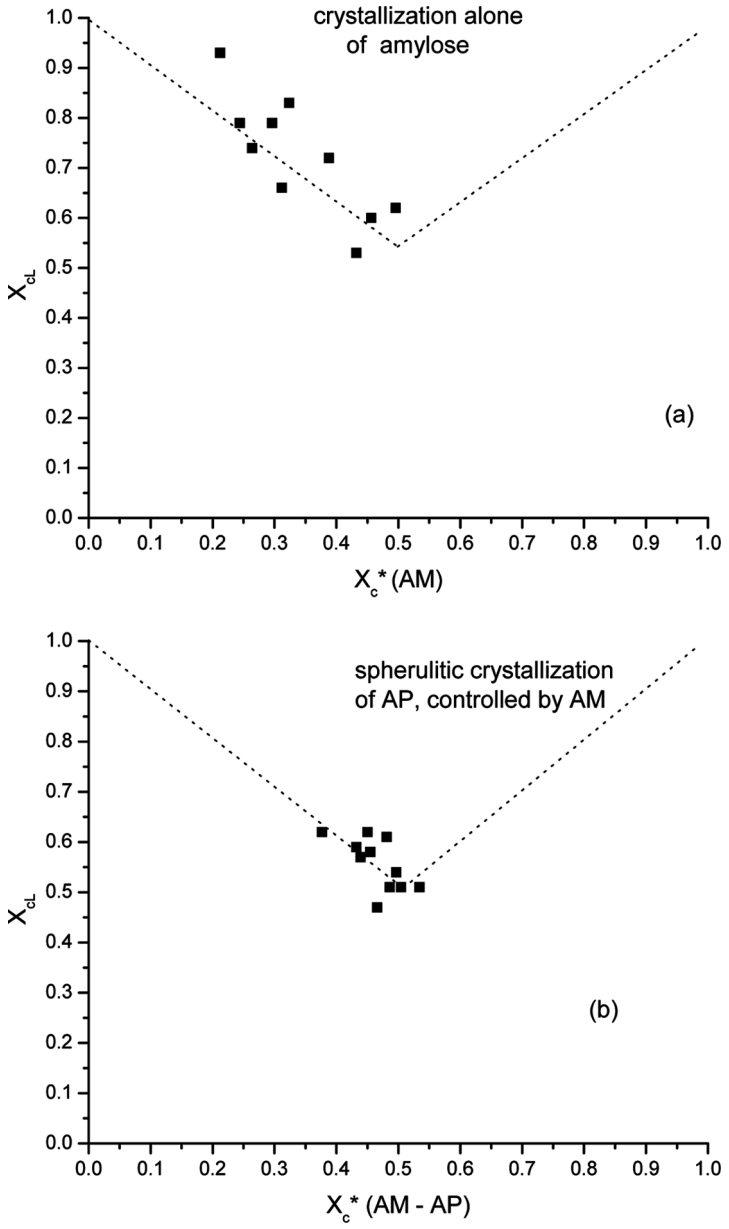

FIGURE 7 X_{cL} data: (a) for the ranges I–III as a function of the degree of crystallinity-X_c^*(AM), referred to the partial volume (0.25) of AM alone; (b) for region IV as a function of the reduced degree of crystallinity of the AM-controlled AP crystal phase.

verification that AM is alone, crystallizing separately in the first step. If all X_{cL} values of the AM crystallization (ranges I–III) are now plotted as a function of the corresponding X_c^* values, it is found that the [1 – X_c^* (AM)] law (see Eq. 2, Figure 5) for X_{cL} is satisfactorily fulfilled (see Figure 7a).

Thus it is concluded that a spherulitic crystallization of AM is observed as presented in beautiful micrographs from Ziegler et al. [18].

This approach can be applied to the second crystallization-mechanism. As pointed out earlier, in this case only one third of the total contribution of AP should be taken into account, that is, the AM controlled nucleation of AP refers to a total volume of 0.25 of AM and 0.25 of AP, that is, a total (AM – AP) volume fraction of 0.5. From Figures 1a and 6 the AM controlled crystallization of AP reaches for $X_c = 0.31$ a value of $X_{cL} = 0.5$. Therefore $X_c^* = 0.31/0.5 = 0.62$. This value is somewhat higher than the expected value of 0.5, suggesting that more than 25% AP of the potato starch is induced to crystallize by AM. Adopting a total fraction of 0.62 for the AM – AP spherulitic crystallization (just compatible with Figure 1b for $X_S X_L$) one obtains X_c^* (AM – AP) = $X_c/0.62$. Hence, X_{cL} (AM – AP) (X_c^*) would extrapolate to 0.5 for $X_c^* = 0.5$, as well (see Figure 7b).

Consequently, instead of a fraction of 25% of the mass of the potato starch according to $0.25/0.75 = 33\%$ of AP, $62\% - 25\% = 37\%$ of the total mass, corresponding to $0.37/0.75 = 49\%$ of AP does crystallize together with AM. Because Figure 7b may be considered as a linear representation, just as that of Figure 7a for AM, the AP crystallized by means of nucleation of AM must contribute to a spherulitic structure, in contrast to the shell-like crystallization of AP molecules without AM nucleation. This AM – AP crystallization nucleates so quickly that its beginning at X_c above 0.12 could not be recorded at the A2 beamline.

Model of AM Controlled-Crystallization of AP

Finally, this article presents some considerations concerning a molecular model of this special kind of AP crystallization. Because AP, contrary to its spherical shell-like structure in native grains, crystallizes like AM, it may be assumed that crystallites within the same spherulite are preformed by the AM crystallization. As the AM did not leave the state of primary crystallization $X_c^*(AM) < 0.5^*$ it is probable that the same occurs for AP: The common crystallization ends up at $X_c = 32\%$, being restricted to 62% of the starch volume. In accordance to $X_c{}^*$(AM – AP) = $0.31/0.62 = 50\%$ the primary crystallization of AM and AP is now completed. The AP crystals may also form radial lamellae, which just fill the radial gaps between the AM lamellae. Optical micrographs

show spherulites in mung bean starch [18]. Some shish kebab structures reveal that lamellae grow perpendicular to the shish axis. This suggests that just as in the case of other linear polymers, molecular chains are vertically oriented to the lamellar surface. Hence, the chains within the AM precrystallization are aligned perpendicularly to the spherulite radius. If one assumes the AP backbone molecule to orient radially from the center (hilum) of the AP molecule, then the outstanding bundles that are capable to crystallize as blocks may form radial lamellae, the chain orientation of them being as in the case of AM. In the molten state, during injection molding, the AP molecule is presumably interpenetrated by the AM network. Hence, upon crystallization there is sufficient material of both starch components within the sphere-shaped volume of the AP star molecule. A joint crystallization may take place within the space of the AP molecule. The center of the mixed spherulite coincides with the center of the AP molecule. However, the spherulite is different from the native spherical-shaped shell AP molecular crystal. Following Reference [19] in this case the backbone is not straight radial but twisted, giving rise to a shell-like structure of twisted lamellae, similar to a banded polyethylene spherulite. The twisting tendency of both, the crystal lamellae and the AP backbone molecule is caused by the chiral construction of the double helices [19]. The flat AM lamellae induce the AP to built up its lamellae in a flat manner too. This explains the influence of the AM on the AP crystallization: Admittedly no common crystals are built up from AM and AP molecules. However, a common spherulite can be formed by lamellae either from AM or from AP. When primary crystallization is completed, the AM and AP crystals may be placed even in an alternating sequence. The spherulite structure is controlled by AM and the diameter of the spherulite is characterized by the size of the AP molecule. One may expect that even amorphous 38% pure AP will also crystallize after a certain delay (see results for the retrogradation of potato starch after 20 days in humid air [17]). The restriction of the retrogradation to $X_c = 32\%$ in this experiment is due to the described AM – AP structure. Only the specially suitable components could crystallize, however, almost completely, except during secondary crystallization. The outstanding crystallization of isolated AP molecules into AP shell crystals is described in Reference [17].

CONCLUSIONS

1. Pure amorphous, injection-molded potato-starch offers a convenient model to examine the early stages of crystallization. Strobl's hypothesis of the block crystallization has been confirmed in

the present case. Individual crystal blocks are formed through water penetration into the blobs of the AM chain, before these can rearrange into lamellae, which on their own may build up a periodic nanostructure.
2. Approximately 25% of the volume of the AM fraction is involved in this first step of crystallization.
3. When the crystallization temperature surpasses 60°C the structure fixed by the secondary network of AM and AP breaks down. Then, owing to a strong penetration of water, further 40% of the volume crystallizes as AP lamellae, which are inserted in between preexisting AM ones.
4. Spherulites consisting of radial lamellae orginating from the centers of the AP molecules are formed. The remnant 40%, that is AP alone, does not crystallize rapidly.
5. After a stepwise temperature increase, in humid atmosphere, up to 94°C, no further crystallization occurred in the experiments.

REFERENCES

[1] Klucinec, J. D. and Thompson, D. B., *Cereal Chemistry* **79** (1), 24 (2002).
[2] Vandeputte, G. E., Vermeylen, R., Geeroms, J., and Delcour, J. A., *J. Cereal Sci*. **38** (1), 61 Jul. (2003).
[3] Rindlav-Westling, A., Stading, M., Hermansson, A. M., and Gatenholm, P., *Carbohydrate Polymers* **36**, 217 (1998).
[4] Bayer, R. K. and Baltá-Calleja, F. J., *J. Macromol. Sci.-Phys*. **44** (4), 471 (2005).
[5] Gidley, M. J., *Macromolecules* **22**, 351 (1989).
[6] Bayer, R. K., Dietrich, F., and Lindemann, S. to be published.
[7] Waigh, T. A., Perry, P., Riekel, C., Gidley, M. J., and Donald, A. M., *Macromolecules* **31**, 7980 (1998).
[8] Bayer, R. K., Zachmann, H. G., Baltá-Calleja, F. J., and Umbach, H., *Polymer Eng. & Sci.* **29** (3), 188 (1989).
[9] Bayer, R. K., Cagiao, M. E., Baltá-Calleja, F. J., *J. of Applied Polymer Sci*. **99**, 180 (2006).
[10] Bayer, R. K., Abdelbaghi, M., and Ania, F. In preparation.
[11] Cagiao, M. E., Bayer, R. K., Rueda, D. R., and Baltá-Calleja, F. J., *J. Appl. Polym. Sci*. **88**, 17 (2003).
[12] Bayer, R. K., *J. Colloid and Polymer Sci*. **272**, 910 (1994).
[13] Heck, B., Hugel, T., Iijima, M., and Strobl, G., *New J. Phys*. **1**, 17.1 (1999).
[14] Bayer, R. K., Dietrich, F., Lindemann, S., and Ania, F. In preparation.
[15] Tateishi, K. and Nakano, A., *Bioscience Biotechnology and Biochemistry* **61** (3), 455 (1997).
[16] Bayer, R. K. and Baltá-Calleja, F. J., *J. Applied Polymer Sci*. in press.
[17] Bayer, R. K. and Baltá-Calleja, F. J. In preparation.
[18] Ziegler, G. R., Creek, J. A., and Runt, J., *Biomacromolecules* **6**, 1547 (2005).
[19] Waigh, T. A., Kato, K. L., Donald, A. M., Gidley, M. J., Clarke, C. J., and Riekel, C., *Starch/Stärke* **52**, 450 (2000).